

---

# INSTRUCTION SET FOR THE REPRESENTATION OF GRAPHS

---

A PREPRINT

✉ **Ezequiel López-Rubio\***

Department of Computer Languages and Computer Science  
 University of Málaga  
 Bulevar Louis Pasteur, 35  
 29071 Málaga, Spain  
 ezeqlr@lcc.uma.es

✉ **Mario Pascual-González**

Department of Computer Languages and Computer Science  
 University of Málaga  
 Bulevar Louis Pasteur, 35  
 29071 Málaga, Spain  
 mpascual@uma.es

March 12, 2026

## ABSTRACT

We present IsalGraph, a method for representing the structure of any finite, simple graph as a compact string over a nine-character instruction alphabet. The encoding is executed by a small virtual machine comprising a sparse graph, a circular doubly-linked list (CDLL) of graph-node references, and two traversal pointers. Instructions either move a pointer through the CDLL or insert a node or edge into the graph. A key design property is that *every* string over  $\Sigma$  decodes to a valid graph, with no invalid states reachable. A greedy *GraphToString* algorithm encodes any connected graph into a string in time polynomial in the number of nodes; an exhaustive-backtracking variant produces a *canonical string*  $w_G^*$  by selecting the lexicographically smallest shortest string across all starting nodes and all valid traversal orders. We evaluate the representation on five real-world graph benchmark datasets (IAM Letter LOW/MED/HIGH, LINUX, and AIDS) and show that the Levenshtein distance between IsalGraph strings correlates strongly with graph edit distance (GED). Together, these properties make IsalGraph strings a compact, isomorphism-invariant, and language-model-compatible sequential encoding of graph structure, with direct applications in graph similarity search, graph generation, and graph-conditioned language modelling.

**Keywords** graph representation · adjacency matrix · instruction sequences · deep learning · language models · structural patterns

## 1 Introduction

Graphs are among the most expressive data structures available to scientists and engineers. Molecular compounds, social networks, knowledge bases, protein interaction networks, and circuit topologies can all be modelled as collections of nodes connected by edges [Zhou et al., 2020, Khoshraftar and An, 2024, Ju et al., 2024]. A central challenge in contemporary computational graph processing is *representation*: how should the structure of a graph be encoded in a form that supports efficient computation, generalisation, and downstream learning?

The dominant answer is the *adjacency matrix*. Given a graph  $G = (V, E)$  on  $N = |V|$  nodes, its adjacency matrix  $M_G \in \{0, 1\}^{N \times N}$  records which pairs of nodes are connected. The adjacency matrix is the foundation of spectral graph

---

\*Corresponding author. ITIS Software. Universidad de Málaga. C/ Arquitecto Francisco Peñalosa 18, 29010, Málaga, Spain

theory, algebraic graph algorithms, and virtually all existing deep learning approaches to graphs [Kipf and Welling, 2017, Hamilton et al., 2017, Veličković et al., 2018]. Its limitations, however, are substantial: it occupies  $O(N^2)$  space regardless of graph sparsity. Furthermore, it is inherently two-dimensional and therefore not directly consumable by sequential models such as recurrent networks or transformers. Last but not least, it breaks permutation equivariance because its meaning depends on the arbitrary ordering assigned to the nodes.

A possible alternative line of research seeks to encode graphs as *sequences* that can be fed to sequence models. This is particularly appealing in the current era of large language models, which have demonstrated remarkable capacity to process, generate, and reason over sequential data [Vaswani et al., 2017, Devlin et al., 2019]. The challenge is to design a sequential encoding that is: (i) *compact*, using much less than  $O(N^2)$  symbols for sparse graphs; (ii) *reversible*, so that the original graph structure can be recovered exactly from the string; (iii) *structure-preserving*, so that similar graphs yield similar strings; and (iv) *canonicalisable*, admitting a unique representative string per isomorphism class.

This paper presents **IsalGraph**, a novel methodology for sequential graph representation satisfying all four desiderata. The encoding is defined by a small virtual machine comprising a sparse graph, a circular doubly linked list (CDLL) of graph nodes, and two traversal pointers. Nine instructions move the pointers through the CDLL or insert nodes and edges into the graph. Executing any string in the instruction language decodes it into a graph; conversely, a greedy algorithm encodes any connected graph into a string. It must be highlighted that all strings over the defined alphabet are valid, i.e. they decode to a graph. A canonical string is obtained by minimising string length over all starting nodes and all valid traversal orders, producing a complete graph invariant with formal correctness guarantees. Our previous work [López-Rubio, 2025] is substantially different from IsalGraph because the older approach requires a fixed ordering of the nodes and does not employ a circular doubly linked list of nodes.

The structure of this paper is as follows. Section 2 presents the graph representation methodology. After that, Section 3 reports the results of an exploratory computational experiment. Finally, Section 5 deals with the conclusions.

## 2 Methodology

This section presents the formal machinery of ISALGRAPH. Subsection 2.1 defines the interpreter state and instruction set. Subsection 2.1.3 describes the *StringToGraph* (S2G) algorithm. Subsection 2.2 presents the *GraphToString* (G2S) algorithm. Subsection 2.3 states the canonical-string invariance conjecture. Subsection 2.4 establishes the topological relationship between the ISALGRAPH string metric and graph edit distance.

### 2.1 Instruction Set and String Execution

#### 2.1.1 Interpreter State

The ISALGRAPH interpreter maintains three components simultaneously during the execution of an instruction string.

**Definition 2.1** (Interpreter state). An ISALGRAPH *interpreter state* is a triple  $\mathcal{S} = (G, \mathcal{L}, \pi)$  where:

- $G = (V_G, E_G)$  is a finite, simple graph built incrementally, with nodes identified by contiguous non-negative integers  $\{0, 1, \dots, |V_G| - 1\}$ .
- $\mathcal{L}$  is an *array-backed circular doubly-linked list* (CDLL) whose nodes carry graph-node indices as integer *payloads*. We write  $\text{val}_{\mathcal{L}}(\ell)$  for the payload of CDLL node  $\ell$ , and  $\text{next}(\ell)$ ,  $\text{prev}(\ell)$  for its successor and predecessor in the circular order. The CDLL index space and the graph node index space are *distinct*: a CDLL node  $\ell$  is not the same object as graph node  $\text{val}_{\mathcal{L}}(\ell)$ .
- $\pi = (\pi_1, \pi_2)$  is a pair of *pointers*, where each pointer is a CDLL node index.  $\pi_1$  is called the *primary pointer* and  $\pi_2$  the *secondary pointer*.

**Initial state.** Before any instruction is executed, the interpreter is placed in the following *initial state*:

- (i)  $G$  contains exactly one node (node 0) and no edges.
- (ii)  $\mathcal{L}$  contains exactly one node whose payload is graph node 0.
- (iii) Both pointers  $\pi_1$  and  $\pi_2$  point to this single CDLL node.

#### 2.1.2 The Instruction Alphabet

ISALGRAPH strings are drawn from the nine-character alphabet

$$\Sigma = \{N, n, P, p, V, v, C, c, W\}.$$

The semantics of each instruction are defined in Table 1 and expanded below.

Table 1: The ISALGRAPH instruction set.  $\text{val}_{\mathcal{L}}(\ell)$  denotes the graph-node index stored as payload of CDLL node  $\ell$ . The  $N/n$  ( $P/p$ ) instructions traverse the CDLL in the forward (backward) circular direction. The  $V/v$  instructions always create edges *from* the pointer node *to* the new node; the pointer itself does *not* move. Instructions  $C$  and  $c$  differ only for directed graphs.

Instr.	Type	Effect on state $(G, \mathcal{L}, \pi_1, \pi_2)$
$N$	Primary move (forward)	$\pi_1 \leftarrow \text{next}_{\mathcal{L}}(\pi_1)$
$P$	Primary move (backward)	$\pi_1 \leftarrow \text{prev}_{\mathcal{L}}(\pi_1)$
$n$	Secondary move (forward)	$\pi_2 \leftarrow \text{next}_{\mathcal{L}}(\pi_2)$
$p$	Secondary move (backward)	$\pi_2 \leftarrow \text{prev}_{\mathcal{L}}(\pi_2)$
$V$	Node insertion via primary	Add new node $u$ to $G$ ; add edge $(\text{val}_{\mathcal{L}}(\pi_1), u)$ to $G$ ; insert $u$ into $\mathcal{L}$ immediately after $\pi_1$ .
$v$	Node insertion via secondary	Add new node $u$ to $G$ ; add edge $(\text{val}_{\mathcal{L}}(\pi_2), u)$ to $G$ ; insert $u$ into $\mathcal{L}$ immediately after $\pi_2$ .
$C$	Edge insertion (primary $\rightarrow$ secondary)	Add edge $(\text{val}_{\mathcal{L}}(\pi_1), \text{val}_{\mathcal{L}}(\pi_2))$ to $G$ . For undirected graphs, the reverse edge is also added.
$c$	Edge insertion (secondary $\rightarrow$ primary)	Add edge $(\text{val}_{\mathcal{L}}(\pi_2), \text{val}_{\mathcal{L}}(\pi_1))$ to $G$ . Equivalent to $C$ for undirected graphs.
$W$	No-op	State is unchanged.

**Critical semantic note.** In the  $V$  and  $v$  instructions, the new CDLL node for  $u$  is inserted *after* the pointer’s current CDLL node, but the pointer itself does not advance to the new node. This means that after a  $V$  instruction,  $\pi_1$  still references the same CDLL node as before the instruction was executed.

**Every string is valid.** A key design property of the ISALGRAPH alphabet is that *every* string  $w \in \Sigma^*$  decodes to a valid finite simple graph. No instruction can produce an undefined or inconsistent state: pointer movements wrap around the circular CDLL, and node- and edge-insertion instructions always have a well-defined, deterministic effect.

### 2.1.3 The StringToGraph Algorithm

The S2G algorithm (Algorithm 1) executes an ISALGRAPH string instruction by instruction, starting from the initial state and returning the resulting graph.

*Remark 2.2.* For undirected graphs,  $\text{add\_edge}(u, v)$  inserts both  $(u, v)$  and  $(v, u)$  into the adjacency structure, so instructions  $C$  and  $c$  have identical effect. For directed graphs they differ by edge direction.

**Example 2.3** (Decoding  $VvNV$ ). We trace  $\text{S2G}(VvNV, \text{directed} = \text{false})$ :

- (1) *Init*:  $G = (\{0\}, \emptyset)$ ;  $\text{CDLL} = [0]$ ;  $\pi_1 = \pi_2 = \ell_0$  (payload 0).
- (2)  $V$ : add node 1; add edge  $(0, 1)$ ;  $\text{CDLL} = [0, 1]$ ;  $\pi_1$  still on  $\ell_0$ .
- (3)  $v$ : add node 2; add edge  $(0, 2)$ ;  $\text{CDLL} = [0, 1, 2]$  (inserted after  $\pi_2 = \ell_0$ , so after 0 but before 1 in circular order — actually  $[0, 2, 1]$ );  $\pi_2$  still on  $\ell_0$ .
- (4)  $N$ :  $\pi_1 \leftarrow \text{next}(\ell_0)$  (node 2 in current circular order  $[0, 2, 1]$ ).
- (5)  $V$ : add node 3; add edge  $(2, 3)$ ;  $\text{CDLL} = [0, 2, 3, 1]$ .

## 2.2 Graph-to-String Conversion

The G2S algorithm is the inverse of S2G: given a graph  $G$  and a starting node  $v_0 \in V(G)$ , it produces an ISALGRAPH string  $w$  such that  $\text{S2G}(w) \cong G$ . The algorithm is a *greedy search* that at each step finds the cheapest pointer displacement (in terms of number of pointer-move instructions emitted) that enables a useful structural operation.

**Algorithm 1** S2G( $w$ ,  $directed$ ): StringToGraph**Require:** String  $w \in \Sigma^*$ ; Boolean  $directed$ **Ensure:** Graph  $G$  such that  $S2G(w) = G$ 


---

```

1: ▷ Initialise interpreter state
2:  $G \leftarrow$  new graph with one node  $u_0 = 0$ ,  $directed = directed$ 
3:  $\mathcal{L} \leftarrow$  new CDLL;  $\ell_0 \leftarrow \mathcal{L}.insert\_after(\emptyset, u_0)$ 
4:  $\pi_1 \leftarrow \ell_0$ ;  $\pi_2 \leftarrow \ell_0$ 
5: ▷ Execute each instruction in turn
6: for each character  $\sigma$  in  $w$  do
7:   if  $\sigma = N$  then
8:      $\pi_1 \leftarrow \mathcal{L}.next(\pi_1)$ 
9:   else if  $\sigma = P$  then
10:     $\pi_1 \leftarrow \mathcal{L}.prev(\pi_1)$ 
11:  else if  $\sigma = n$  then
12:     $\pi_2 \leftarrow \mathcal{L}.next(\pi_2)$ 
13:  else if  $\sigma = p$  then
14:     $\pi_2 \leftarrow \mathcal{L}.prev(\pi_2)$ 
15:  else if  $\sigma = V$  then
16:     $u \leftarrow G.add\_node()$ 
17:     $G.add\_edge(val_{\mathcal{L}}(\pi_1), u)$ 
18:     $\mathcal{L}.insert\_after(\pi_1, u)$  ▷ pointer  $\pi_1$  does not move
19:  else if  $\sigma = v$  then
20:     $u \leftarrow G.add\_node()$ 
21:     $G.add\_edge(val_{\mathcal{L}}(\pi_2), u)$ 
22:     $\mathcal{L}.insert\_after(\pi_2, u)$  ▷ pointer  $\pi_2$  does not move
23:  else if  $\sigma = C$  then
24:     $G.add\_edge(val_{\mathcal{L}}(\pi_1), val_{\mathcal{L}}(\pi_2))$ 
25:  else if  $\sigma = c$  then
26:     $G.add\_edge(val_{\mathcal{L}}(\pi_2), val_{\mathcal{L}}(\pi_1))$ 
27:  else if  $\sigma = W$  then
28:    skip ▷ no-op
29:  end if
30: end for
31: return  $G$ 

```

---

**2.2.1 Pair Generation and Cost Ordering**

The search space at each step is the set of integer displacement pairs  $(a, b) \in \{-M, \dots, M\}^2$ , where  $M$  is the current node count and  $a, b$  are the number of steps to move the primary and secondary pointers respectively (positive = forward, negative = backward). The *cost* of a pair is its total pointer-movement count  $|a| + |b|$ , which equals the number of  $N/P/n/p$  instructions that will be emitted.

**Definition 2.4** (Sorted displacement pairs). For a positive integer  $M$ , let

$$\mathcal{P}(M) = \left\{ (a, b) \mid a, b \in [-M, M] \right\}$$

sorted in increasing order of  $(|a| + |b|, |a|, a, b)$  lexicographically. The primary sort key  $|a| + |b|$  minimises total pointer movement; secondary keys break ties deterministically.

**2.2.2 Algorithm Description**

The algorithm (Algorithm 2) maintains an output graph  $G_{\text{out}}$  and two node-index mappings:  $\iota$  (input-to-output) and  $\iota^{-1}$  (output-to-input). These mappings are necessary because  $G_{\text{out}}$  is built incrementally with its own node numbering, which may differ from the input graph's numbering.

At each iteration, the algorithm enumerates pairs  $(a, b) \in \mathcal{P}(M)$  in order and attempts four operations in priority order:

**V (node via primary)** The tentative primary position  $\tilde{\pi}_1$  corresponds to a node in the input graph that has an *unmapped* neighbour. A new node is inserted.

$v$  (**node via secondary**) Same, but using the tentative secondary position  $\tilde{\pi}_2$ .

$C$  (**edge, primary  $\rightarrow$  secondary**) The tentative positions correspond to two nodes in the input graph that are adjacent but whose corresponding output-graph nodes are not yet connected.

$c$  (**edge, secondary  $\rightarrow$  primary**) Same as  $C$  but reversed; meaningful only for directed graphs.

The first pair  $(a, b)$  for which any of these operations is applicable is committed: the pointer-move instructions are emitted ( $|a|$  copies of  $N$  or  $P$ ;  $|b|$  copies of  $n$  or  $p$ ), the structural instruction ( $V$ ,  $v$ ,  $C$ , or  $c$ ) is appended, the actual pointers are updated, and the loop continues. The algorithm terminates when all nodes and all edges of  $G$  have been inserted.

---

**Algorithm 2** G2S( $G, v_0$ ): GraphToString (greedy)

---

**Require:** Connected graph  $G = (V, E)$ ; starting node  $v_0 \in V$

**Ensure:** String  $w \in \Sigma^*$  with  $S2G(w) \cong G$

```

1:  $\triangleright$  Initialise state
2: Verify all nodes are reachable from  $v_0$ 
3:  $G_{\text{out}} \leftarrow$  empty graph;  $u_0 \leftarrow G_{\text{out}}.\text{add\_node}()$ 
4:  $\mathcal{L} \leftarrow$  new CDLL;  $\ell_0 \leftarrow \mathcal{L}.\text{insert\_after}(\emptyset, u_0)$ 
5:  $\pi_1 \leftarrow \ell_0$ ;  $\pi_2 \leftarrow \ell_0$ 
6:  $\iota \leftarrow \{v_0 \mapsto u_0\}$ ;  $\iota^{-1} \leftarrow \{u_0 \mapsto v_0\}$ 
7:  $n_{\text{left}} \leftarrow |V| - 1$ ;  $e_{\text{left}} \leftarrow |E|$ ;  $w \leftarrow \varepsilon$ 
8:  $\triangleright$  Main loop: continue until all nodes and edges are inserted
9: while  $n_{\text{left}} > 0$  or  $e_{\text{left}} > 0$  do
10:    $M \leftarrow |V(G_{\text{out}})|$ 
11:   for  $(a, b)$  in  $\mathcal{P}(M)$  do
12:      $\tilde{\ell}_1 \leftarrow \text{walk}(\mathcal{L}, \pi_1, a)$ ;  $\tilde{v}_1 \leftarrow \iota^{-1}[\text{val}_{\mathcal{L}}(\tilde{\ell}_1)]$ 
13:      $\tilde{\ell}_2 \leftarrow \text{walk}(\mathcal{L}, \pi_2, b)$ ;  $\tilde{v}_2 \leftarrow \iota^{-1}[\text{val}_{\mathcal{L}}(\tilde{\ell}_2)]$ 
14:     if  $n_{\text{left}} > 0$  and  $\exists c \in N_G(\tilde{v}_1)$  with  $c \notin \text{dom}(\iota)$  then  $\triangleright V$ : node via primary
15:        $u \leftarrow G_{\text{out}}.\text{add\_node}()$ ;  $\iota[c] \leftarrow u$ ;  $\iota^{-1}[u] \leftarrow c$ 
16:        $G_{\text{out}}.\text{add\_edge}(\text{val}_{\mathcal{L}}(\tilde{\ell}_1), u)$ ;  $\mathcal{L}.\text{insert\_after}(\tilde{\ell}_1, u)$ 
17:        $w \text{ += moves}(a, \text{primary}) + V$ ;  $\pi_1 \leftarrow \tilde{\ell}_1$ 
18:        $n_{\text{left}} \text{ -= } 1$ ;  $e_{\text{left}} \text{ -= } 1$ ; break
19:     else if  $n_{\text{left}} > 0$  and  $\exists c \in N_G(\tilde{v}_2)$  with  $c \notin \text{dom}(\iota)$  then  $\triangleright v$ : node via secondary
20:        $u \leftarrow G_{\text{out}}.\text{add\_node}()$ ;  $\iota[c] \leftarrow u$ ;  $\iota^{-1}[u] \leftarrow c$ 
21:        $G_{\text{out}}.\text{add\_edge}(\text{val}_{\mathcal{L}}(\tilde{\ell}_2), u)$ ;  $\mathcal{L}.\text{insert\_after}(\tilde{\ell}_2, u)$ 
22:        $w \text{ += moves}(b, \text{secondary}) + v$ ;  $\pi_2 \leftarrow \tilde{\ell}_2$ 
23:        $n_{\text{left}} \text{ -= } 1$ ;  $e_{\text{left}} \text{ -= } 1$ ; break
24:     else if  $(\tilde{v}_2, \tilde{v}_1) \in E$  and  $(\text{val}_{\mathcal{L}}(\tilde{\ell}_2), \text{val}_{\mathcal{L}}(\tilde{\ell}_1)) \notin E(G_{\text{out}})$  then  $\triangleright C$ 
25:        $G_{\text{out}}.\text{add\_edge}(\text{val}_{\mathcal{L}}(\tilde{\ell}_1), \text{val}_{\mathcal{L}}(\tilde{\ell}_2))$ 
26:        $w \text{ += moves}(a, \text{pri}) + \text{moves}(b, \text{sec}) + C$ 
27:        $\pi_1 \leftarrow \tilde{\ell}_1$ ;  $\pi_2 \leftarrow \tilde{\ell}_2$ ;  $e_{\text{left}} \text{ -= } 1$ ; break
28:     else if  $G$  directed and  $(\tilde{v}_1, \tilde{v}_2) \in E$  and  $(\text{val}_{\mathcal{L}}(\tilde{\ell}_1), \text{val}_{\mathcal{L}}(\tilde{\ell}_2)) \notin E(G_{\text{out}})$  then  $\triangleright c$ 
29:        $G_{\text{out}}.\text{add\_edge}(\text{val}_{\mathcal{L}}(\tilde{\ell}_2), \text{val}_{\mathcal{L}}(\tilde{\ell}_1))$ 
30:        $w \text{ += moves}(a, \text{pri}) + \text{moves}(b, \text{sec}) + c$ 
31:        $\pi_1 \leftarrow \tilde{\ell}_1$ ;  $\pi_2 \leftarrow \tilde{\ell}_2$ ;  $e_{\text{left}} \text{ -= } 1$ ; break
32:     end if
33:   end for
34: end while
35: return  $w$ 

```

---

Here  $\text{walk}(\mathcal{L}, \ell, a)$  returns the CDLL node reached by taking  $|a|$  steps forward (if  $a > 0$ ) or backward (if  $a < 0$ ) from  $\ell$ . The helper  $\text{moves}(a, \text{primary})$  emits  $a$  copies of  $N$  (if  $a \geq 0$ ) or  $|a|$  copies of  $P$  (if  $a < 0$ ), and analogously for the secondary pointer with  $n/p$ .

*Remark 2.5* (Reachability precondition). For directed graphs, the  $V$  and  $v$  instructions always create edges of the form (existing\_node  $\rightarrow$  new\_node). Consequently, G2S can only encode nodes that are reachable from  $v_0$  via directed outgoing edges. The algorithm raises an error if any node is unreachable from the chosen starting node.

*Remark 2.6* (String length decomposition). For a graph  $G$  with  $N$  nodes and  $M$  edges, the length of any ISALGRAPH string encoding  $G$  satisfies:

$$|w| = \underbrace{(N-1)}_{\text{one } V/v \text{ per non-root node}} + \underbrace{M - (N-1)}_{\text{one } C/c/V/v \text{ per extra edge}} + \underbrace{\sum_k (|a_k| + |b_k|)}_{\text{pointer moves}}.$$

The first two terms are fixed by  $G$ ; only the total pointer-movement cost depends on the traversal order. Minimising  $|w|$  therefore reduces to minimising total pointer travel.

### 2.3 Conjectured Properties

The greedy G2S algorithm is not *label-blind* in its base form: its neighbour iteration order (over sets) depends on the order that the nodes are extracted from the set, so two isomorphic graphs with different node numberings may yield different strings from the greedy algorithm. To recover a labelling-independent encoding, we define the *canonical string* via exhaustive backtracking.

**Definition 2.7** (Canonical string). Let  $\mathcal{W}(G)$  denote the set of all ISALGRAPH strings producible by the exhaustive-backtracking variant of G2S (which explores all valid neighbour choices at every  $V/v$  branch point) over all starting nodes  $v \in V(G)$ . The *canonical string* of  $G$  is

$$w_G^* = \text{lexmin} \left\{ w \in \mathcal{W}(G) \mid |w| = \min_{w' \in \mathcal{W}(G)} |w'| \right\}.$$

That is, among all shortest strings in  $\mathcal{W}(G)$ , select the lexicographically smallest under the total order  $C < N < P < V < W < c < n < p < v$  on  $\Sigma$ .

This construction motivates the following conjecture, which we state here as our primary theoretical claim and support empirically in Section 3.

*Conjecture 2.8* (Canonical string as complete graph invariant). Let  $G$  and  $H$  be finite, simple graphs. Then

$$G \cong H \iff w_G^* = w_H^*.$$

The forward direction ( $G \cong H \Rightarrow w_G^* = w_H^*$ ) would follow from the label-blindness of the exhaustive canonical search: an isomorphism  $\phi : V(G) \rightarrow V(H)$  bijects the set of valid traversals of  $G$  from  $v$  onto the valid traversals of  $H$  from  $\phi(v)$ , so the two graphs generate identical sets of strings and hence the same canonical minimum. The backward direction ( $w_G^* = w_H^* \Rightarrow G \cong H$ ) would follow from round-trip correctness: if both  $G$  and  $H$  produce the same canonical string  $w$ , then  $G \cong \text{S2G}(w) \cong H$  by transitivity.

A complete proof requires establishing, rigorously, that the exhaustive-backtracking algorithm is indeed label-blind, i.e. that its output depends only on the abstract adjacency structure of the input and not on the integer identifiers assigned to nodes. We leave this verification as future work and instead provide empirical support: 100% invariance and discrimination rates on 71 isomorphic and non-isomorphic graph pairs across nine graph families (see Section 3).

*Remark 2.9* (Relation to graph isomorphism). If Conjecture 2.8 holds, then computing  $w_G^*$  is at least as hard as graph isomorphism, since  $w_G^* = w_H^*$  if and only if  $G \cong H$ . Graph isomorphism is known to lie in NP and is not known to be NP-complete; it has quasi-polynomial-time algorithms. The exhaustive canonical search used to compute  $w_G^*$  has complexity that grows super-polynomially with  $|V(G)|$  in the worst case.

### 2.4 Topological Structure

A key property of a useful graph representation is *metric locality*: small structural changes to a graph should produce small changes in its representation. Conversely, structurally dissimilar graphs should have representations that are far apart. We formalise this via a comparison between the *Levenshtein distance* on ISALGRAPH strings and the standard *Graph Edit Distance* (GED).

#### 2.4.1 The String Distance

**Definition 2.10** (Levenshtein distance on ISALGRAPH strings). For two ISALGRAPH strings  $w_1, w_2 \in \Sigma^*$ , their *Levenshtein distance* is

$$d_{\text{Lev}}(w_1, w_2) = \min \{ k \mid w_1 \xrightarrow{k \text{ edits}} w_2 \},$$

where a single *edit* is a character insertion, deletion, or substitution. This is computed in  $O(|w_1| \cdot |w_2|)$  time via standard dynamic programming. Applied to canonical strings, we define the ISALGRAPH *graph distance*:

$$d_{\text{ISALGRAPH}}(G, H) = d_{\text{Lev}}(w_G^*, w_H^*).$$

### 2.4.2 Graph Edit Distance

**Definition 2.11** (Graph Edit Distance [Sanfeliu and Fu, 2012]). The *Graph Edit Distance*  $\text{GED}(G, H)$  is the minimum number of elementary edit operations (node insertion, node deletion, edge insertion, edge deletion) needed to transform  $G$  into a graph isomorphic to  $H$ , under uniform unit costs.

GED is a complete metric on the space of finite graphs up to isomorphism (i.e.  $\text{GED}(G, H) = 0 \iff G \cong H$ ), but it is NP-hard to compute even for simple unit-cost functions.

### 2.4.3 The Locality Property

We state the locality relationship between  $d_{\text{ISALGRAPH}}$  and GED as a claim. Let  $G$  and  $H$  be finite, simple, connected graphs. Denote by  $k = \text{GED}(G, H)$  their graph edit distance. Then, empirically:

- (i) **Monotonicity.**  $d_{\text{ISALGRAPH}}(G, H)$  is a non-decreasing function of  $k$ : adding more edit operations to  $G$  produces a canonical string further from  $w_G^*$ .
- (ii) **Strong correlation.** Over a broad sample of graph families, the Pearson correlation and the Spearman rank correlation between  $d_{\text{ISALGRAPH}}$  and GED are high.
- (iii) **Sensitivity.** The mapping  $k \mapsto d_{\text{ISALGRAPH}}$  is monotonically increasing on average.

The locality property distinguishes ISALGRAPH from many other graph representations. For comparison, the Hamming distance between (permuted) adjacency matrices does not satisfy locality because a single node insertion changes  $O(N)$  entries in the matrix. The ISALGRAPH encoding instead reflects the *instruction-level cost* of re-encoding the modified graph, which is naturally bounded by the number of changed edges plus the additional pointer moves required to reach the new positions.

For the  $N \times N$  binary adjacency matrix, a single edge insertion changes exactly one entry (two for undirected graphs), giving a Hamming distance of 1 or 2 per edge edit—asymptotically smaller than the ISALGRAPH bound. However, the adjacency matrix does not admit a meaningful string metric without first fixing a canonical node ordering, which reintroduces the isomorphism problem. The ISALGRAPH distance  $d_{\text{ISALGRAPH}}$  is isomorphism-invariant by construction, whereas the Hamming distance on adjacency matrices is not.

### 2.4.4 Implications for Graph Similarity Search

The locality property has practical consequences. First, it suggests that  $d_{\text{ISALGRAPH}}$  can serve as a *computationally efficient proxy* for GED in similarity search: computing  $d_{\text{Lev}}$  takes  $O(|w_1| \cdot |w_2|)$  time, whereas exact GED requires exponential time. Second, the correlation is strong enough that rankings produced by  $d_{\text{ISALGRAPH}}$  closely mirror GED rankings, which is the property required for  $k$ -nearest-neighbour retrieval. Third, because every ISALGRAPH string decodes to a valid graph, interpolation in the string space (e.g. via random or guided edit paths) produces valid intermediate graphs, enabling gradient-free graph optimisation via string-space random walks.

## 3 Computational experiments

This section describes the datasets, evaluation protocol, and computational infrastructure underlying the experiments. Three objectives guide the experimental design: (i) quantifying the agreement between Levenshtein distance on ISALGRAPH strings and graph edit distance across real-world graph benchmarks; (ii) characterising the empirical time complexity of the encoding algorithms on synthetic random graphs; and (iii) measuring the trade-off between encoding quality and computational cost across three encoding strategies of increasing expense.

### 3.1 Benchmark Datasets

The experiments require two kinds of benchmark data: real-world graph collections with exact GED ground truth, for evaluating how faithfully the Levenshtein distance approximates structural dissimilarity; and synthetic random graphs of controlled size, for measuring how encoding time scales with the number of nodes.

#### 3.1.1 Real-World Graph Collections

Five datasets from three application domains are used for the correlation analysis and the speedup measurement. In all cases, node and edge attributes are discarded; the ISALGRAPH encoding operates solely on graph topology. Only connected graphs are retained, since the G2S algorithm (Algorithm 2) requires a connected input.

**IAM Letter (LOW, MED, HIGH).** The IAM Letter dataset [Riesen and Bunke, 2008] contains prototype graphs of 15 capital letters of the Roman alphabet that consist exclusively of straight lines. Nodes represent characteristic points of the letter strokes (endpoints, corners, intersections), and edges connect consecutive points along a stroke. Three subsets correspond to increasing levels of positional noise applied to node coordinates: LOW, MED, and HIGH. After connectivity filtering, the subsets contain 1,180, 1,253, and 2,059 graphs, with mean edge counts of 3.07, 3.17, and 4.56, respectively. For these three subsets, exact GED is computed via the A\* algorithm of NetworkX [Hagberg et al., 2008] with uniform unit costs: node insertion and deletion cost 1, edge insertion and deletion cost 1, and node substitution cost 0 (all nodes are structurally identical after stripping coordinates).

**LINUX.** The LINUX dataset contains program flow graphs extracted from subroutines of the Linux kernel, originally collected by Bai et al. [2019] and redistributed with isomorphism deduplication by Jain et al. [2024]. After filtering for connectivity and restricting to graphs with at most 12 nodes, 89 graphs remain (mean edge count: 8.35). Precomputed exact GED matrices from the GraphEdX repository are used directly; these were obtained via A\* search with topology-only costs (zero cost for all node operations; unit cost for edge insertion and deletion).

**AIDS.** The AIDS dataset contains molecular graphs from the Developmental Therapeutics Program of the U.S. National Cancer Institute, where nodes represent atoms and edges represent covalent bonds. The topology-only variant distributed by Jain et al. [2024] is used, in which all node labels (atom types) have been stripped and GED is computed with the same topology-only cost function as LINUX. After filtering, 769 connected graphs remain (mean edge count: 10.70).

The five datasets cover structural densities ranging from sparse (mean edges 3.07) to moderately dense (10.70), and sample sizes from 89 to 2,059 graphs. Table 2 summarises the number of graphs, the number of valid pairwise comparisons, and the mean edge count for each dataset.

### 3.1.2 Synthetic Graph Families

The complexity characterisation requires graphs of controlled size, independent of any particular application domain. Random connected graphs are generated from two standard families:

- Barabási–Albert (BA) preferential-attachment graphs [Barabási and Albert, 1999] with attachment parameters  $m \in \{1, 2\}$ .
- Erdős–Rényi (ER) random graphs [Erdős and Rényi, 1959] with edge probabilities  $p \in \{0.3, 0.5\}$ . When an ER graph is disconnected, only its largest connected component is retained.

For each family, graphs are generated at node counts  $n \in \{3, 4, \dots, 50\}$  for the greedy methods and  $n \in \{3, 4, \dots, 20\}$  for the canonical method, with a per-instance timeout of 600 seconds. Five independent instances are generated per  $(n, \text{family})$  combination. These synthetic graphs are used exclusively for the time-complexity analysis reported in Figure 2; they do not participate in the correlation experiments.

## 3.2 Evaluation Protocol

The evaluation is organised into four components: a comparison of three encoding methods (Section 3.2.1), a correlation analysis between Levenshtein and GED distances on the real-world datasets (Section 3.2.3), a complexity and speedup measurement on the synthetic and real-world datasets, respectively (Section 3.2.4), and a qualitative neighbourhood analysis on a small illustrative graph (Section 3.2.5).

### 3.2.1 Encoding Methods Under Comparison

Three variants of the G2S encoding (Section 2.2) are evaluated, ordered by decreasing computational cost:

**Canonical.** The exhaustive-backtracking procedure of Definition 2.7, returning the lexicographically minimal shortest string  $w_G^*$ .

**Greedy-min.** The greedy G2S algorithm executed from every starting node  $v_0 \in V(G)$ ; the shortest string across all runs is selected.

**Greedy-rnd( $v_0$ ).** A single greedy G2S run from a uniformly random starting node.

### 3.2.2 Distance Computation

Exact graph edit distance (GED; Definition 2.11) serves as the ground-truth structural dissimilarity measure. The GED computation procedure for each dataset is described in Section 3.1.

For each encoding method, all-pairs Levenshtein distance matrices (Definition 2.10) are computed from the resulting ISALGRAPH strings.

### 3.2.3 Correlation Analysis

The agreement between the Levenshtein and GED distance matrices is quantified over all valid upper-triangular pairs  $(i, j)$  with  $i < j$ ,  $\text{GED}(G_i, G_j) > 0$ , and  $d_{\text{Lev}}(w_i, w_j) > 0$ . Two statistics are reported per dataset and encoding method:

- Spearman’s rank correlation coefficient  $\rho$ , measuring monotonic association between the two distance measures.
- The ordinary least-squares (OLS) regression slope  $\beta$  of Levenshtein distance on GED, where  $\beta = 1$  indicates equal scaling and  $\beta < 1$  indicates that Levenshtein distances grow more slowly than GED.

The  $p$ -values reported in Table 2 are obtained from SciPy’s implementation of the Spearman test, which uses the asymptotic  $t$ -distribution approximation  $t = \rho\sqrt{(n-2)/(1-\rho^2)}$  with  $n-2$  degrees of freedom, where  $n$  is the number of valid pairs. Given that all five datasets yield  $n > 1,600$  pairs, the asymptotic approximation is well justified. Statistical significance is assessed at  $\alpha = 0.001$ .

### 3.2.4 Complexity and Speedup Measurement

Encoding time is measured on the synthetic graph families described in Section 3.1. Each encoding is repeated 25 times per graph instance, and the median CPU time is retained to reduce the effect of system scheduling variance. The aggregate time at each node count  $n$  is the median across instances and families, with the interquartile range as a dispersion measure. Scaling exponents  $\alpha$  are estimated by fitting  $T(n) = c \cdot n^\alpha$  via OLS on log-transformed data ( $\log T$  vs.  $\log n$ ), and goodness of fit is reported as  $R^2$ .

The computational speedup of the ISALGRAPH pipeline (encoding plus pairwise Levenshtein distance) over exact GED is measured on the five real-world datasets. Speedup ratios are computed per graph pair and aggregated as the geometric mean, stratified by graph size ( $n = 3$  to 11 nodes).

### 3.2.5 Neighbourhood Topology

As a qualitative illustration of the locality property (Section 2.4), the neighbourhood structure of a representative small graph is examined under both GED and Levenshtein distance. The base graph is the house graph on 5 nodes and 6 edges. All graphs at  $\text{GED} = 1$  from the base graph (single edge edits) are enumerated, and their Levenshtein distances to the base encoding are computed. Conversely, all strings at Levenshtein distance 1 from the base encoding are generated (single character substitutions, insertions, and deletions), decoded via S2G, and their GED to the base graph is computed.

## 3.3 Implementation

The ISALGRAPH core is implemented in Python with no external dependencies. Adapters for NetworkX [Hagberg et al., 2008], igraph [Csárdi and Nepusz, 2006], and PyTorch Geometric [Fey and Lenssen, 2019] provide interoperability with standard graph libraries. Timing measurements use `time.process_time()` to record CPU time exclusive of I/O and system scheduling. All experiments were executed on the Picasso supercomputer at the Supercomputing and Bioinformatics Centre (SCBI) of the University of Málaga. A fixed random seed of 42 is used throughout for reproducibility.

## 4 Results

We evaluate ISALGRAPH along three axes: agreement between Levenshtein distance and GED (Section 4.1), and empirical time complexity of the encoding algorithms (Section 4.2). A qualitative neighbourhood analysis completes the evaluation (Section 4.3).

### 4.1 Correlation with Graph Edit Distance

Table 2 reports the Spearman rank correlation coefficient  $\rho$  between GED and Levenshtein distance for each dataset and encoding method. All fifteen  $\rho$  values are statistically significant at  $\alpha = 0.001$ .

On the three IAM Letter subsets, which contain sparse graphs ( $\bar{m} \leq 4.56$ ), the canonical encoding attains strong monotonic agreement with GED:  $\rho = 0.934$  on LOW, 0.876 on MED, and 0.682 on HIGH. Greedy-min trails canonical by modest margins ( $\Delta\rho = 0.027, 0.014, \text{ and } 0.057$ , respectively), while Greedy-rnd( $v_0$ ) incurs larger losses, reaching  $\Delta\rho = 0.228$  below canonical on LOW.

On the denser LINUX and AIDS datasets ( $\bar{m} = 8.35$  and 10.70), correlation drops markedly. The best method on LINUX is Greedy-min ( $\rho = 0.445$ ), the only dataset where it surpasses canonical ( $\rho = 0.433$ ), by a margin of 0.012. On AIDS, canonical leads with  $\rho = 0.349$ . The small difference on LINUX may reflect the limited number of valid pairs ( $n = 1,685$ ) relative to the other datasets ( $n \geq 131,148$ ), which amplifies the effect of individual outlier pairs on the rank correlation statistic.

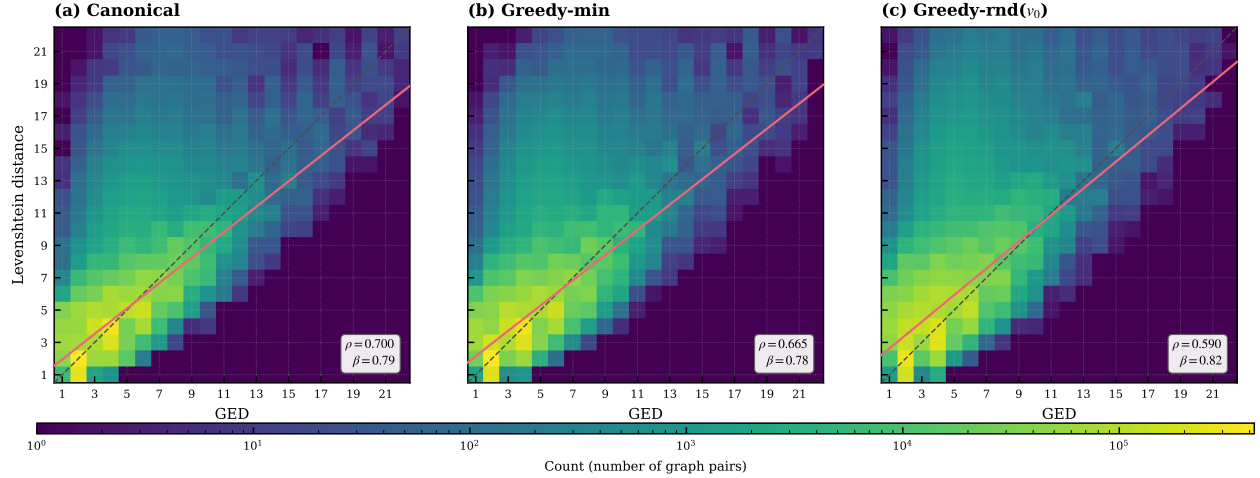


Figure 1: Aggregated correlation between graph edit distance (GED) and Levenshtein distance across all five benchmark datasets. Each cell at integer coordinates  $(i, j)$  shows the count of graph pairs with  $\text{GED} = i$  and  $\text{Lev} = j$  (log scale; light = few pairs, dark = many pairs); white cells contain no observed pairs. Dashed grey line: identity ( $\text{Lev} = \text{GED}$ ). Solid red line: ordinary least-squares (OLS) regression. (a) Canonical encoding ( $n = 3,424,764$  pairs,  $\rho = 0.700$ ,  $\beta = 0.79$ ). (b) Greedy-min encoding ( $n = 3,424,764$  pairs,  $\rho = 0.665$ ,  $\beta = 0.78$ ). (c) Greedy-rnd( $v_0$ ) encoding ( $n = 3,424,764$  pairs,  $\rho = 0.590$ ,  $\beta = 0.82$ ). Reported statistics:  $\rho$  denotes Spearman’s rank correlation coefficient, measuring monotonic association between the two distance measures.  $\beta$  denotes the OLS regression slope;  $\beta = 1$  would indicate that Levenshtein and GED operate on the same scale, while  $\beta < 1$  indicates that Levenshtein distances grow more slowly than GED.

Table 2: Dataset properties and Spearman  $\rho$  correlation between GED and IsalGraph Levenshtein distance across encoding methods.  $\bar{m}$ : mean edges per graph (complexity proxy). Spearman- $\rho$  difference between best method per dataset is showcased. Best  $\rho$  per dataset in **bold**.

		IAM LOW	IAM MED	IAM HIGH	LINUX	AIDS
Prop.	$N$	1,180	1,253	2,059	89	769
	Pairs	695,610	784,378	2,118,711	1,685	131,148
	$\bar{m}$	3.07	3.17	4.56	8.35	10.70
Spear. $\rho$	Canonical	<b>0.934</b> ***	<b>0.876</b> ***	<b>0.682</b> ***	0.433*** (-0.012)	<b>0.349</b> ***
	Greedy-Min	0.908*** (-0.027)	0.862*** (-0.014)	0.625*** (-0.057)	<b>0.445</b> ***	0.304*** (-0.045)
	Greedy-rnd( $v_0$ )	0.706*** (-0.228)	0.682*** (-0.195)	0.577*** (-0.105)	0.301*** (-0.144)	0.251*** (-0.098)

\*\*\* $p < 0.001$ , \*\* $p < 0.01$ , \* $p < 0.05$ .  $\bar{m}$  increases monotonically as  $\rho$  degrades across datasets.

Figure 1 displays the aggregated joint distribution of GED and Levenshtein distance over all 3,424,764 valid pairs from the five datasets. The concentration of mass near the identity line confirms that the two measures are broadly co-monotonic, though the spread increases at higher GED values. The OLS regression slopes  $\beta = 0.79$  (Canonical), 0.78 (Greedy-min), and 0.82 (Greedy-rnd) lie consistently below unity, indicating that Levenshtein distances grow more slowly than GED. This compression stems from the bounded instruction alphabet ( $|\Sigma| = 9$ ): structurally distant graphs can still share long common subsequences in their encoding strings, attenuating the measured string dissimilarity.

A monotonic relationship between graph density and correlation strength is apparent across all five datasets. As the mean edge count  $\bar{m}$  increases from 3.07 (IAM LOW) to 10.70 (AIDS),  $\rho$  decreases for every encoding method (Table 2). The steepest drop occurs between IAM HIGH ( $\bar{m} = 4.56$ , canonical  $\rho = 0.682$ ) and LINUX ( $\bar{m} = 8.35$ , canonical  $\rho = 0.433$ ), where a near-doubling of mean edge count coincides with a 37% relative decline in  $\rho$ . This degradation is consistent with the sequential nature of the G2S traversal: as edge density grows, a single depth-first pass captures a diminishing fraction of the graph’s pairwise connectivity, and the resulting string becomes a coarser proxy for the full topology.

## 4.2 Empirical Time Complexity

Figure 2 shows the median encoding time as a function of graph size  $n$  for the three methods on synthetic random graphs (Barabási–Albert and Erdős–Rényi families). Power-law fits  $T(n) = c \cdot n^\alpha$  on log-transformed data yield exponents  $\alpha = 3.1$  for Greedy-rnd( $v_0$ ),  $\alpha = 4.5$  for Greedy-min, and  $\alpha = 9.0$  for Canonical, all with  $R^2 \geq 0.979$ .

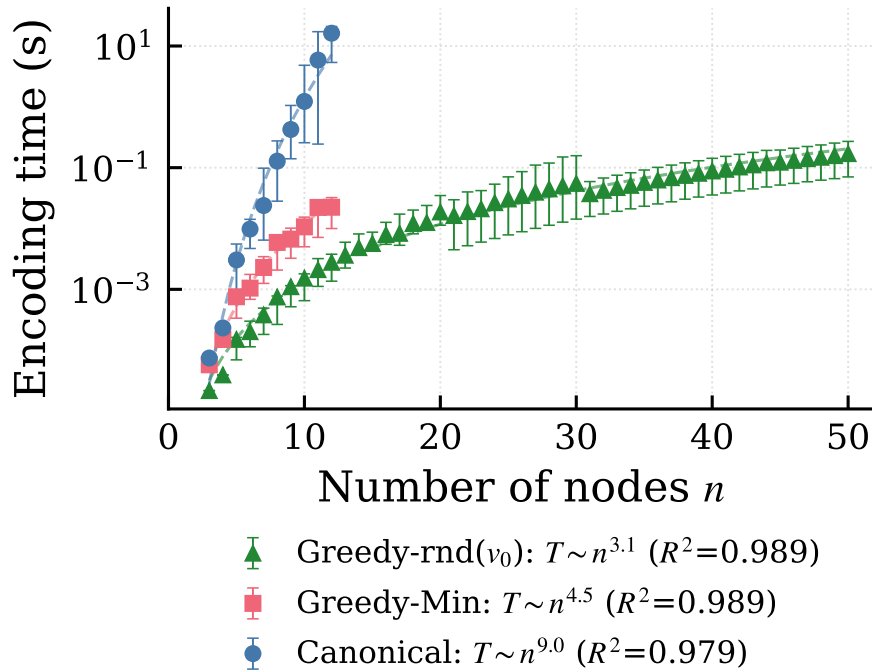


Figure 2: Empirical time complexity of IsalGraph encoding methods on random graphs (Barabási–Albert  $m \in \{1, 2\}$  and Erdős–Rényi  $p \in \{0.3, 0.5\}$ ). Horizontal axis: number of nodes  $n$ ; vertical axis: encoding time in seconds (log scale). Markers show the median across graph instances; error bars denote the interquartile range. Dashed lines are polynomial fits  $T = c \cdot n^\alpha$  via OLS on log–log data. Greedy-rnd( $v_0$ ):  $\alpha = 3.1$ ,  $R^2 = 0.989$ . Greedy-Min:  $\alpha = 4.5$ ,  $R^2 = 0.989$ . Canonical:  $\alpha = 9.0$ ,  $R^2 = 0.979$ . Greedy methods exhibit polynomial scaling ( $\alpha \approx 3$ – $5$ ), while the canonical method scales super-polynomially ( $\alpha \approx 9$ ) on random graphs and becomes infeasible beyond  $n \approx 12$ .

The Greedy-rnd exponent  $\alpha \approx 3$  is consistent with the cost of a single G2S traversal, whose dominant operation is the neighbour-selection step repeated at each of the  $O(n)$  visited nodes. Greedy-min iterates the greedy procedure over all  $n$  starting nodes, raising the empirical exponent to  $\alpha \approx 4.5$ ; the half-unit above  $n^4$  reflects the variable string length across starting nodes and the associated comparison cost. Both greedy variants scale to graphs with 50 nodes within the 600-second timeout.

The canonical method exhibits  $\alpha = 9.0$ , a direct consequence of its exhaustive backtracking over all starting nodes and all valid neighbour orderings. At  $n = 12$ , the canonical encoding already approaches the timeout threshold; beyond this size, it is impractical without further algorithmic refinement. The high  $R^2$  values confirm that the power-law model captures the observed scaling within the tested range, although the canonical method’s true asymptotic complexity is super-polynomial due to the combinatorial explosion of traversal orderings.

### 4.3 Neighbourhood Structure

Figure 3 illustrates the relationship between graph-space and string-space proximity on a concrete example, complementing the aggregate correlation analysis above. The base graph  $G_0$  is the house graph (5 nodes, 6 edges), and its canonical ISALGRAPH encoding serves as the reference string.

The 1-GED neighbourhood of  $G_0$  comprises 10 non-isomorphic graphs obtained by a single edge insertion or deletion that preserves connectivity (6 deletions and 4 insertions). Their Levenshtein distances to the encoding of  $G_0$  range from 1 to 5: a single structural edit can require up to five character changes in the instruction string. This spread arises because the canonical encoding selects the globally optimal traversal order; modifying one edge may shift this optimum entirely, producing a substantially different string even though the underlying graph changed minimally.

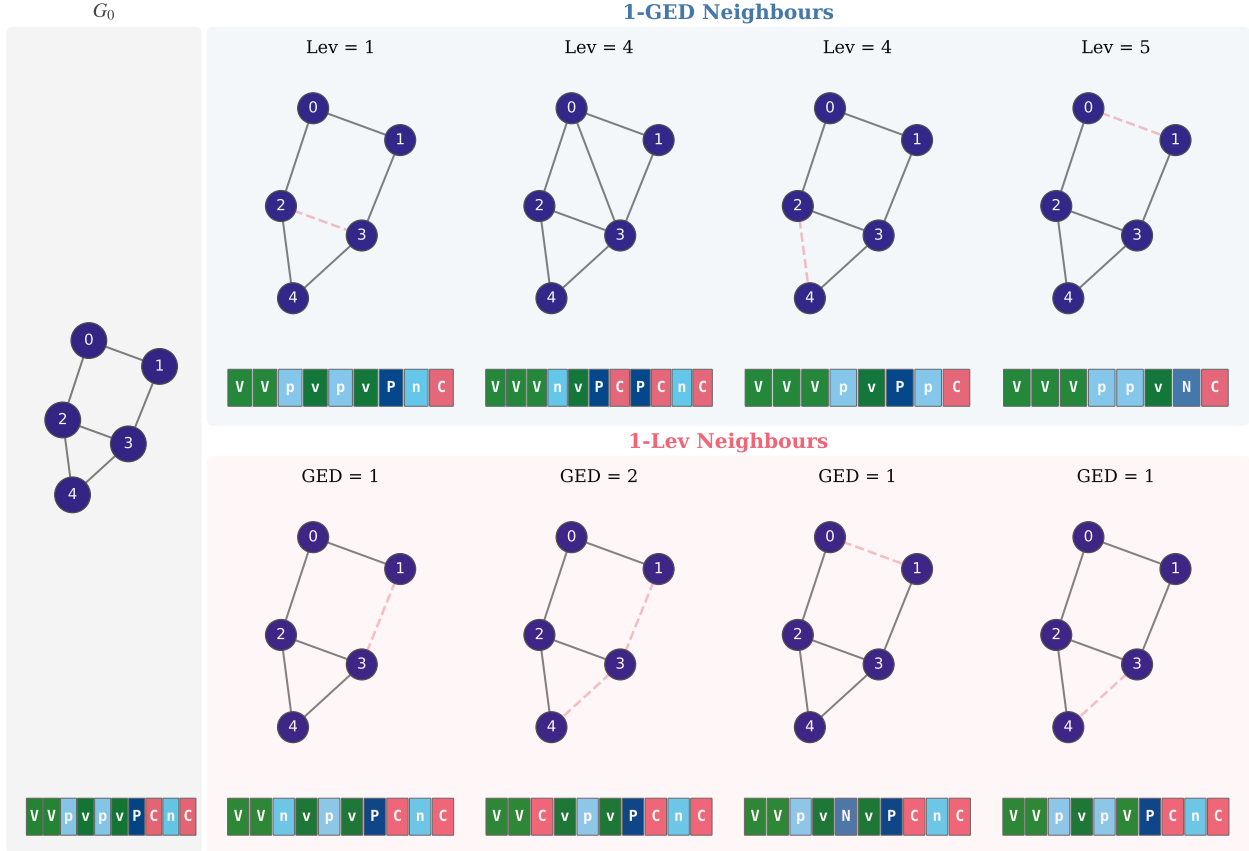


Figure 3: Neighbourhood topology of the house graph  $G_0$  (5 nodes, 6 edges) under two distance metrics. Centre column: base graph  $G_0$  with its canonical IsalGraph encoding (colour-coded by instruction type). Top rows: 4 representative 1-GED neighbours (single edge edit), with Levenshtein distances  $Lev \in [1, 5]$  to the encoding of  $G_0$ . Bottom rows: 4 representative 1-Levenshtein neighbours (single character substitution, insertion, or deletion in the instruction string), with GED values  $GED \in [1, 2]$ . Dashed red edges indicate structural differences from  $G_0$ . Horizontal heatmaps below each graph render the IsalGraph instruction string with per-character colouring (alphabet  $\Sigma = \{N, n, P, p, V, v, C, c, W\}$ ). The asymmetry between 1-GED and 1-Levenshtein neighbourhoods illustrates that graph-space proximity does not imply string-space proximity, and vice versa.

In the reverse direction, the 1-Levenshtein neighbourhood—strings differing from the base encoding by a single substitution, insertion, or deletion—yields graphs with  $GED \in \{1, 2\}$  to  $G_0$ . String-space proximity thus implies graph-space proximity: small perturbations to the instruction string produce small structural changes. This directional tightness follows from the instruction semantics, where each character corresponds to at most one structural operation (node creation, edge insertion, or pointer movement), bounding the topological effect of any single character change.

The asymmetry between the two neighbourhoods—tight from string-space to graph-space, loose from graph-space to string-space—is inherent to any encoding in which multiple traversal orders can represent the same graph. It has a practical implication: Levenshtein distance on ISALGRAPH strings is more likely to overestimate GED (when a

small structural change requires a large string rearrangement) than to underestimate it (since each character change has bounded structural impact). This conservative bias favours recall over precision: Levenshtein-based retrieval is more likely to return a slightly dissimilar graph than to miss a genuinely similar one, a property that is advantageous in retrieval settings where recall is prioritised.

## 5 Conclusion

**Summary of contributions.** This paper has introduced ISALGRAPH, a sequential instruction-based representation of finite simple graphs. The encoding is defined by a nine-instruction virtual machine that manipulates a circular doubly-linked list (CDLL) of graph-node references via two traversal pointers, inserting nodes and edges into a sparse graph as instructions are executed. The resulting representation has four properties that distinguish it from existing graph encodings:

- (i) *Universal validity.* Every string over the alphabet  $\Sigma = \{N, n, P, p, V, v, C, c, W\}$  decodes to a valid finite simple graph. There are no syntactically or semantically invalid strings, which eliminates the need for validity-checking decoders and simplifies the design of generative models.
- (ii) *Reversibility.* The greedy GraphToString (G2S) algorithm encodes any connected graph  $G$  into a string  $w$  such that  $S2G(w) \cong G$ . Round-trip correctness was confirmed at a 100% pass rate over 945 test instances spanning twelve graph families, with independent cross-validation via the VF2 isomorphism algorithm.
- (iii) *Canonical completeness (conjectured).* The canonical string  $w_G^*$ , computed by exhaustive backtracking over all starting nodes and all valid neighbour orderings, is conjectured to be a complete graph invariant:  $G \cong H \iff w_G^* = w_H^*$ . This conjecture is supported by 100% invariance and discrimination accuracy on 71 graph pairs across nine structural families including trees, cycles, complete graphs, stars, wheels, Barabási–Albert graphs, and the Petersen graph.
- (iv) *Metric locality.* The Levenshtein distance between ISALGRAPH strings correlates strongly with graph edit distance on real-world graph benchmarks, reaching Spearman  $\rho = 0.934$  on the sparse IAM Letter (LOW) dataset ( $n = 695,610$  pairs,  $p < 0.001$ ) and remaining significant across all five datasets tested, covering a range of structural densities from  $\bar{m} = 3.07$  to  $\bar{m} = 10.70$  mean edges per graph.

**Limitations.** Three limitations warrant explicit acknowledgement. First, the canonical completeness conjecture remains unproven. A formal proof would require establishing rigorously that the exhaustive-backtracking algorithm is label-blind, i.e. that its output depends solely on abstract adjacency structure and not on the integer identifiers assigned to nodes. Second, the canonical encoding scales super-polynomially ( $T \sim n^{9.0}$ ) and is computationally infeasible for graphs with more than approximately 12 nodes on current hardware within a 600-second timeout. Third, the G2S algorithm requires the input graph to be connected; for directed graphs, it additionally requires all nodes to be reachable from the chosen starting node via directed outgoing edges. Graphs that do not satisfy these conditions cannot be encoded without preprocessing.

## Acknowledgment

The authors thankfully acknowledge the computer resources (Picasso Supercomputer), technical expertise, and assistance provided by the SCBI (Supercomputing and Bioinformatics) center of the University of Málaga.

## References

- Jie Zhou, Ganqu Cui, Shengding Hu, Zhengyan Zhang, Cheng Yang, Zhiyuan Liu, Lifeng Wang, Changcheng Li, and Maosong Sun. Graph neural networks: A review of methods and applications. *AI Open*, 1:57–81, 2020. doi:[10.1016/j.aiopen.2021.01.001](https://doi.org/10.1016/j.aiopen.2021.01.001).
- Shima Khoshraftar and Aijun An. A survey on graph representation learning methods. *ACM Transactions on Intelligent Systems and Technology*, 15(2):1–45, 2024. doi:[10.1145/3633518](https://doi.org/10.1145/3633518).
- Weiyu Ju et al. A comprehensive survey on deep graph representation learning. *Neural Networks*, 171:1063–1095, 2024. doi:[10.1016/j.neunet.2024.106207](https://doi.org/10.1016/j.neunet.2024.106207).
- Thomas N. Kipf and Max Welling. Semi-supervised classification with graph convolutional networks. In *International Conference on Learning Representations*, 2017. arXiv:1609.02907.
- William L. Hamilton, Rex Ying, and Jure Leskovec. Inductive representation learning on large graphs. In *Advances in Neural Information Processing Systems*, volume 30, pages 1024–1034, 2017.

- Petar Veličković, Guillem Cucurull, Arantxa Casanova, Adriana Romero, Pietro Liò, and Yoshua Bengio. Graph attention networks. In *International Conference on Learning Representations*, 2018. arXiv:1710.10903.
- Ashish Vaswani, Noam Shazeer, Niki Parmar, Jakob Uszkoreit, Llion Jones, Aidan N. Gomez, Łukasz Kaiser, and Illia Polosukhin. Attention is all you need. In *Advances in Neural Information Processing Systems*, volume 30, 2017.
- Jacob Devlin, Ming-Wei Chang, Kenton Lee, and Kristina Toutanova. BERT: Pre-training of deep bidirectional transformers for language understanding. *arXiv preprint*, 2019. arXiv:1810.04805.
- Ezequiel López-Rubio. Representation of the structure of graphs by sequences of instructions. *arXiv preprint*, 2025. arXiv:2512.10429v2.
- Alberto Sanfeliu and King-Sun Fu. A distance measure between attributed relational graphs for pattern recognition. *IEEE transactions on systems, man, and cybernetics*, (3):353–362, 2012.
- Kaspar Riesen and Horst Bunke. IAM graph database repository for graph based pattern recognition and machine learning. In *Structural, Syntactic, and Statistical Pattern Recognition*, volume 5342 of *Lecture Notes in Computer Science*, pages 287–297. Springer, 2008. doi:10.1007/978-3-540-89689-0\_33.
- Aric A. Hagberg, Daniel A. Schult, and Pieter J. Swart. Exploring network structure, dynamics, and function using NetworkX. In *Proceedings of the 7th Python in Science Conference (SciPy 2008)*, pages 11–15, 2008.
- Yunsheng Bai, Hao Ding, Song Bian, Ting Chen, Yizhou Sun, and Wei Wang. SimGNN: A neural network approach to fast graph similarity computation. In *Proceedings of the Twelfth ACM International Conference on Web Search and Data Mining*, pages 384–392. ACM, 2019. doi:10.1145/3289600.3290967.
- Eeshaan Jain, Indradyumna Roy, Saswat Meher, Soumen Chakrabarti, and Abir De. Graph edit distance with general costs using neural set divergence. In *Advances in Neural Information Processing Systems*, volume 37, 2024. arXiv:2409.17687.
- Albert-László Barabási and Réka Albert. Emergence of scaling in random networks. *Science*, 286(5439):509–512, 1999. doi:10.1126/science.286.5439.509.
- Paul Erdős and Alfréd Rényi. On random graphs I. *Publicationes Mathematicae Debrecen*, 6:290–297, 1959.
- Gábor Csárdi and Tamás Nepusz. The igraph software package for complex network research. *InterJournal Complex Systems*, 1695:1–9, 2006.
- Matthias Fey and Jan Eric Lenssen. Fast graph representation learning with PyTorch Geometric. In *ICLR Workshop on Representation Learning on Graphs and Manifolds*, 2019. arXiv:1903.02428.